Annals of Biomedical Engineering, Vol. 32, No. 10, October 2004 (© 2004) pp. 1365–1383

Adaptive Predictive Control of Arterial Blood Pressure Based on a Neural Network during Acute Hypotension

KOJI KASHIHARA,[1,2] TORU KAWADA,[1] KAZUNORI UEMURA,[1] MASARU SUGIMACHI,[1] and KENJI SUNAGAWA[1]

[1]Department of Cardiovascular Dynamics, National Cardiovascular Center Research Institute, 5-7-1 Fujishirodai, Suita, Osaka 565-8565, Japan and [2]The Organization for Pharmaceutical Safety and Research, Shin-Kasumigaseki Building, 3-3-2 Kasumigaseki, Chiyoda, Tokyo 100-0013, Japan

(Received 7 August 2003; accepted 20 May 2004)

Abstract—In acute hypotension, an automated drug infusion system to control mean arterial blood pressure (MAP) has not been previously studied, though many investigations have examined the use of vasodilating drugs to control MAP in postoperative hypertension. Therefore, we examined an automated control of MAP during acute hypotension using a neural network (NN) approach. A proportional-integral-derivative (PID) control, an adaptive predictive control using a NN (APC_{NN}), a combined control of APC_{NN} and PID ($APC_{NN\text{-}PID}$), a fuzzy control, and a model predictive control were tested in computer simulation based on the MAP response to norepinephrine (NE) of 25 μg ml^{-1}. In six anesthetized rabbits, using the NE of 25 μg ml^{-1}, the PID control, APC_{NN}, and $APC_{NN\text{-}PID}$ prevented severe hypotension compared to an uncontrolled condition. Under PID control, four of the six animals showed MAP oscillation. Using NE of 50 μg ml^{-1}, the rabbits recovered from acute hypotension for all systems tested but showed sustained MAP oscillation during PID control. In conclusion, utilization of a NN for adaptive predictive control systems could facilitate the development of an automated drug infusion apparatus because it provides robust control even when acute or large perturbations and inter-individual differences in the sensitivity to therapeutic agents occur.

Keywords—Automated drug infusion system, Norepinephrine, Rabbits, Proportional-integral-derivative control.

INTRODUCTION

In a clinical setting, it is necessary to regulate many physiological parameters in the presence of disturbances including interactions among therapeutic agents, unexpected and acute changes in hemodynamic variables, and background noise.[9] Many investigators have reported on the use of automated drug infusion systems using vasodilators in postoperative hypertension[13,18,28] and multiple drug infusion systems to regulate hemodynamics such as cardiac output and mean arterial blood pressure (MAP).[9,22] However, in acute hypotension, an automated drug infusion system to control MAP has not been studied previously because no controller was robust enough to handle the associated unexpected large disturbances and complex modeling of various pathological states. If a system could be designed, which adapted to acute hypotension, and combined with a multiple drug infusion system,[9,22] it would be useful for application in a clinical setting.

Catecholamines, fluid infusion, and blood transfusion are required to maintain local circulation to vital organs during acute hypotension.[3,6,26] The catecholamines contribute to the quick recovery of MAP from a state of acute hypotension.[20,31] However, the sensitivity or responsiveness to the pharmacological agents generally differs among patients, and even within the same individual, the effects of pharmacological intervention could vary with time due to changes in a patient's underlying pathophysiology.[2] Further, the dose-response relationship is usually nonlinear, which makes a prediction of MAP response difficult. The cumulative effects of the past intervention on the current MAP[29] also complicate MAP control. Therefore, proper drug infusion for MAP control largely relies on the expertise of anesthesiologists and clinicians. Developing a reliable method for automating the drug infusion system would improve a patient's individualized drug therapy and minimize the total amount of drug required, which may allow an early tapering off of the drug.

Automated drug infusion systems for controlling MAP have been constructed previously using proportional-integral-derivative (PID) algorithms.[19,27] As long as the MAP response to pharmacological intervention does not change markedly, simple control with PID-tuned parameters works reasonably well. However, the PID controller cannot achieve maximum performance in all situations because of the nonlinear time-varying MAP response and the differences of drug sensitivity among patients.[1,13,34] To overcome the limitation of PID control, adaptive MAP controls have been developed to provide consistent

Address correspondence to Koji Kashihara, Department of Cardiovascular Dynamics, National Cardiovascular Center Research Institute, 5-7-1 Fujishirodai, Suita, Osaka 565-8565, Japan. Electronic mail: kasihara@ri.ncvc.go.jp

0090-6964/04/1000-1365/1

performance. These adaptive controllers recursively update their own parameters so as to compensate for both the time-varying characteristics of MAP response and the intra- and inter-individual differences to drug sensitivity.[18,28,33] Because the conventional adaptive controls still rely on a moment-to-moment linearity in MAP response to drug infusion, they might not be able to adapt to the nonlinear MAP response when large perturbations such as acute and severe hypotension[1] occur.

A neural network (NN) is a useful tool that can identify and learn nonlinear time-varying systems even in the presence of intra- and inter-individual variability in a patient's vital signs with large perturbations.[15,30] Therefore, an adaptive predictive control based on a NN (APC_{NN}) may be more robust compared to the conventional PID controller in stabilizing the system in the presence of nonlinearities in patient response and sensitivities to a drug.[1,11,17] The purpose of the present study was to explore the utility of a MAP control system based on an APC_{NN} algorithm. One limitation of using an advanced algorithm is that the added computational expense results in longer times for system identification compared to a simpler algorithm such as PID control. To overcome this performance limitation, we also constructed an APC_{NN} combined with PID control ($APC_{NN\text{-}PID}$). The performance of the APC_{NN} and $APC_{NN\text{-}PID}$ systems was compared to that of a traditional PID system, using a hemorrhage-induced acute hypotension condition to alter MAP. To estimate the effects of the simple adaptive control using artificial intelligence or the predictive control compared with APC_{NN} or $APC_{NN\text{-}PID}$, we tested the PID control based on fuzzy inference or model predictive control (MPC). Finally, we tested the robustness of each system, to control MAP, using two different concentrations of a vasopressor agent, norepinephrine (NE), at concentrations of 25 and 50 μg ml^{-1}.

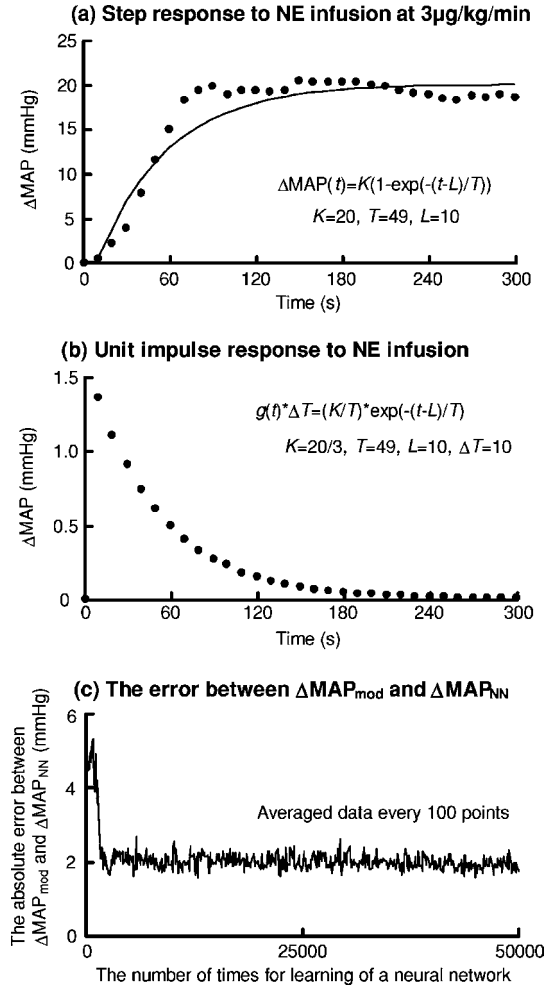

FIGURE 1. (a) Step response to norepinephrine (NE) infusion at 3 μg kg^{-1} min^{-1}, (b) Unit impulse response to NE infusion, (c) The absolute error between actual changes in mean arterial blood pressure ($\Delta MAP(t)$) as the model ($\Delta MAP_{mod}(t)$) and $\Delta MAP_{NN}(t)$ showing predicted changes in MAP by a neural network (NN).

METHODS

Modeling of MAP Response

To make a simple model for MAP response to a drug infusion, we obtained the average step response as MAP changed from baseline (ΔMAP) during a 5-min NE infusion at 3 μg kg^{-1} min^{-1} in anesthetized rabbits ($n = 3$) without hemorrhage [Fig. 1(a)]. The ΔMAP response (sampling rate = 10 Hz) was averaged every 10 s. We approximated the step response of ΔMAP to the following first-order delay system with a pure time delay:

$$\Delta\mathrm{MAP}(t) = \begin{cases} K \cdot \left[1 - \exp\left(-\dfrac{t-L}{T}\right)\right] & (t \geq L) \\ 0 & (t < L) \end{cases} \quad (1)$$

where K is a proportional gain [mmHg (μg kg^{-1} min^{-1})$^{-1}$], T is a time constant (s), and L is the pure time delay (s). $K = 20$, $T = 49$, and $L = 10$ were acquired from the approximation of the averaged step response [Fig. 1(a)].

The ΔMAP response as a model (ΔMAP_{mod}) was calculated by the convolution integral in the discrete-time domain as follows:

$$\Delta\mathrm{MAP}_{\mathrm{mod}}(t) = \sum_{\tau=0}^{N_m} g(\tau) \cdot \Delta T \cdot u(t-\tau) \quad (2)$$

where

$$g(t) = \frac{K}{T} \cdot \exp\left(-\frac{t-L}{T}\right)$$

$u(t)$ is the infusion rate of NE (μg kg^{-1} min^{-1}) and $g(t)$ is the unit impulse response (mmHg). The $g(t)$ is calculated from the derivative values of the step response of Eq. (1) [Fig. 1(b)]. ΔT is the sampling interval (s) and N_m is the finite number of terms in the model for the unit impulse response.

K is a proportional gain [mmHg (μg kg^{-1} min^{-1})$^{-1}$], T is a time constant (s), and L is the pure time delay (s). The parameters of ΔMAP_{mod} were $\Delta T = 10$, $N_m = 30$, $K = 20/3$, $T = 49$, and $L = 10$.

Design of Controllers

PID Control

We applied the PID algorithm as a velocity form algorithm. The velocity form algorithm determines the drug infusion rate rather than the total amount of drug infused. The algorithm can be expressed in the discrete time domain as follows [Fig. 2(a)],[4]

$$\Delta u(t) = K_P \cdot \left\{ [e(t) - e(t-1)] + \frac{\Delta T}{T_I} \cdot e(t) + \frac{T_D}{\Delta T} \cdot [e(t) - 2 \cdot e(t-1) + e(t-2)] \right\} \quad (3)$$

$$u(t) = u(t-1) + \Delta u(t)$$

where $u(t)$ = NE infusion rate (μg kg^{-1} min^{-1}), $\Delta u(t)$ = change in $u(t)$, K_P = proportional gain [(μg kg^{-1} min^{-1}) mmHg^{-1}], T_I = integral time (s), T_D = derivative time (s), ΔT = sampling interval (10 s), $e(t)$ = difference (mmHg) between a target value and observed MAP at a given time. PID parameters were determined by the Ziegler–Nichols[36] method, resulting in $K_P = 0.3$, $T_I = 20$, and $T_D = 5$.

Adaptive Predictive Control Based on a NN (APC_{NN})

Figure 2(b) shows a block diagram of an APC_{NN} system. The APC_{NN} is a control system where the NN shown in Fig. 3 recursively learns the characteristics of a patient using their observed ΔMAP response to NE infusion, and then determines the predicted output after N_p steps. First, in the closed loop controls, the NN learned about ΔMAP response only once every 10 s to prevent overlearning of ΔMAP during rapid disturbances or artifacts ["1. Learning Loop" in Fig. 2(b) and (c)]. Second, the learned ΔMAP_{NN} response was used for the prediction of future ΔMAP responses by the NN ["2. Prediction Loop" in Fig. 2(b) and (c)]. The initial connection weights for the NN were determined from the learning-stage results using the ΔMAP_{mod} [see Eq. (2)].

Feed-Forward Output Using a NN. Figure 3 shows the components of a NN. A multilayer feed-forward NN with two hidden layers was used to emulate the ΔMAP_{mod} response. The NN structure used was a nonlinear autoregressive moving average (NARMA) model[1,32] as follows:

$$\Delta MAP_{NN}(t) = f(\Delta MAP(t-1), u(t-1), u(t-2), u(t-3), u(t-4), u(t-5), u(t-6)) \quad (4)$$

where $\Delta MAP_{NN}(t)$ is the MAP change estimated by the NN. $\Delta MAP(t-1)$ is the actual MAP change induced by NE infusion before one sampling interval (10 s) has passed. The input layer in a NN is composed of the past input and output. The duration of past NE infusion rate was set to 1 min accounting for the pure time delay in the ΔMAP response differing among patients.

The input values are sent through the first hidden layer, second hidden layer, and output layer (see Feed-Forward Output Using a NN under Appendix). When the NN calculates the output, the hyperbolic tangent function is applied 14 times (7 in the first hidden layer and 7 in the second hidden layer).

Backpropagation Algorithm for Learning. To identify the MAP response and determine the initial weights in a NN for MAP controls, the NN was trained using the output of the ΔMAP_{mod} response to random inputs. In the present study, we used the backpropagation algorithm in the online mode as follows.

All connection weights are adjusted to decrease the error function by the backpropagation learning rule based on the gradient descent method.[24,25] The error function, E is as follows:

$$E = \frac{1}{2} \cdot \varepsilon^2 = \frac{1}{2} \cdot [\Delta MAP - \Delta MAP_{NN}]^2 \quad (5)$$

where ΔMAP is the actual MAP change as a supervised signal, ΔMAP_{NN} is the ΔMAP predicted by the NN before update of the connection weights, and ε is the difference between ΔMAP and ΔMAP_{NN}. The ΔMAP_{NN} predicted by a NN is compared with the actual ΔMAP, and its error is calculated by Eq. (5). The error is back propagated through the network, and the connection weight is generally updated by the gradient descent of E as a function of the weights.[30]

$$w^* = w + Kn \cdot \Delta w \quad (6)$$

where

$$\Delta w = \frac{\partial E}{\partial w} = \frac{\partial E}{\partial \varepsilon} \cdot \frac{\partial \varepsilon}{\partial MAP_{NN}} \cdot \frac{\partial MAP_{NN}}{\partial w} = -\varepsilon \cdot \frac{\partial MAP_{NN}}{\partial w},$$

w^* is the weight of each connection after update, w is the weight of each connection before update, Δw is the modified weight, K_n is the learning rate.

In the present study, the backpropagation algorithm was performed in the following order: output layer, second hidden layer, and first hidden layer (see Backpropagation Algorithm for Learning under Appendix). The total number of weights in the NN was 120 (105 for layer weights and 15 for bias, Fig. 3). The combination of a fixed input $x_0 = 1$ and an extra input weight w_0 is known as a bias input (Fig. 3[1,30]).

Determination of Initial Weights in a NN. To determine the initial weights in the NN for the APC_{NN} and $APC_{NN\text{-}PID}$, we made the NN learn the ΔMAP_{mod} response. The starting

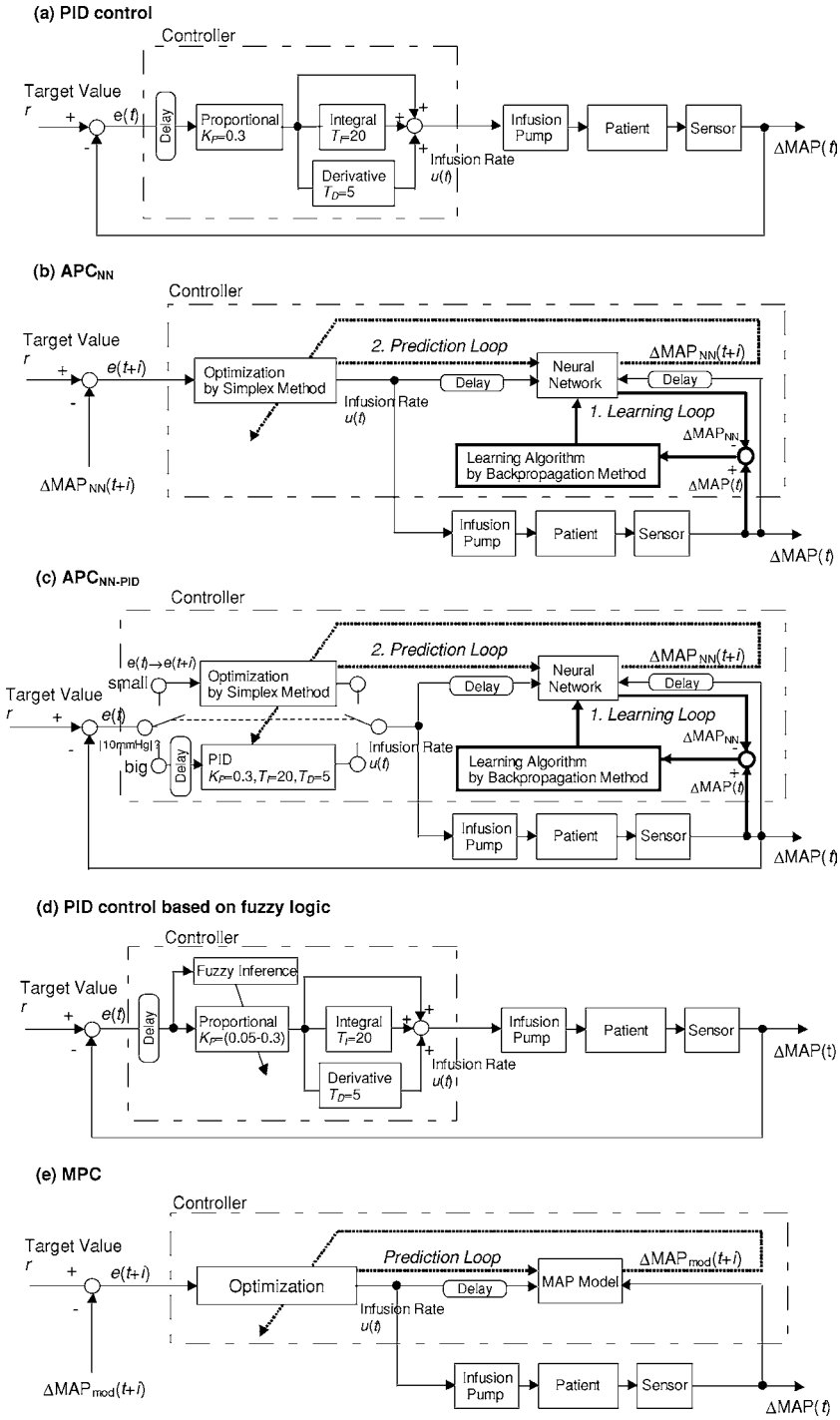

FIGURE 2. The block diagram for a MAP control system. (a) A proportional-integral-derivative (PID) control. (b) An adaptive predictive control using a neural network (APC$_{NN}$). (c) APC$_{NN}$ combined with PID control (APC$_{NN-PID}$). (d) PID control based on fuzzy inference. (e) Model predictive control (MPC). *u* (*t*): infusion rate of NE.*r*: a target value. *e* (*t*): error between the target value and observed MAP. *e* (*t* + *i*): error between the target value and MAP predicted by the NN (ΔMAP$_{NN}$(*t* + *i*)) or the model MAP response (ΔMAP$_{mod}$(*t* + *i*)). ΔMAP(*t*), ΔMAP$_{NN}$, and ΔMAP$_{NN}$(*t* + *i*) are actual changes in MAP, MAP changes by the NN before update, and changes in MAP predicted by the NN, respectively.

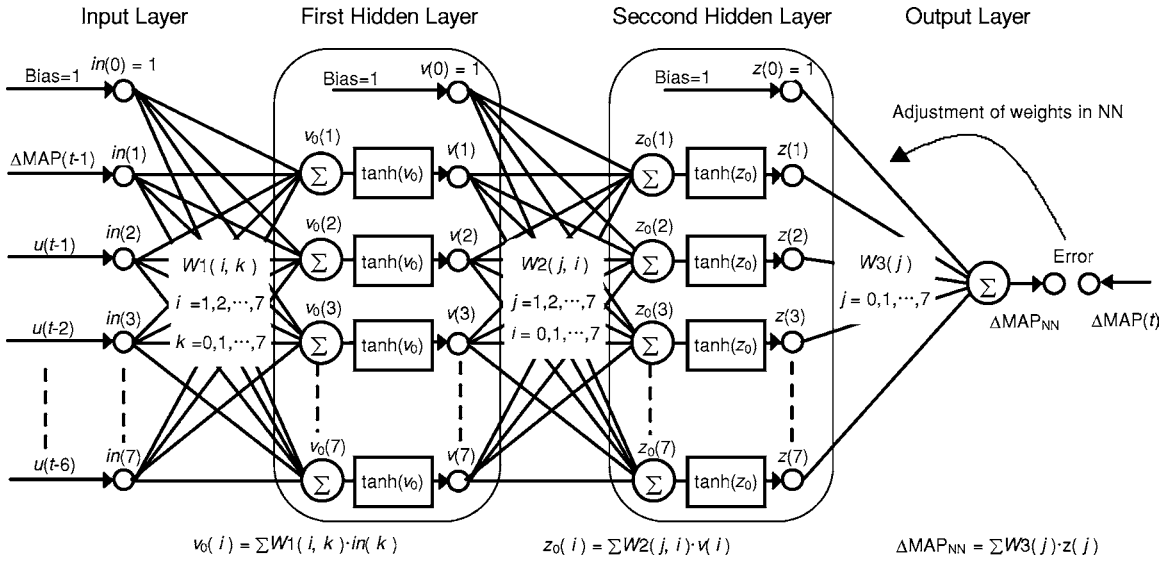

FIGURE 3. A four-layer feed-forward NN with two hidden layers to emulate the characteristics of a patient. The number of units in each hidden layer of the NN was set to seven (the same number as the input units). The NN had the unit bias. A hyperbolic tangent function [tanh(*x*)] was used as the output of each unit.

weights in the NN before the learning of the ΔMAP_{mod} response were assigned at random between -1 and 1. Then, the infusion rate of NE at $-4 \leq u(t) \leq 6$ μg kg^{-1}min^{-1} was assigned at random and learning calls were replicated 50,000 times.[30] The ΔMAP_{mod} response during the learning process contained random noise between 0 and -5. Then, normalization was performed by dividing all outputs by 50 and the fixed learning rate was $K_n = 0.1$, which showed the most suitable number determined by a trial and error approach. This learning rate was smaller than that used for the actual MAP controls because it was necessary to avoid a local minimum.[25]

The absolute error between the ΔMAP_{mod} and the ΔMAP_{NN} response from the trained NN are shown in Fig. 1(c). Because of the random noise between 0 and -5, which emulated the hypotensive disturbances, the learning result of the NN showed an error of approximately 2 mmHg compared with the ΔMAP_{mod} data. The trained NN was used for the following simulation and animal studies, and the learning rate of the NN was set to $K_n = 0.2$ under the studies in order to quickly converge to the target value.[24,25,30]

As shown in Fig. 4(a), the goal of the APC_{NN} was to calculate the optimal NE infusion rate, $u(t)$, which minimized the following cost function [$J(t)$],

$$J(t) = \sum_{i=1}^{N_p} [r(t+i) - \Delta MAP_{NN}(t+i)]^2 \qquad (7)$$

where N_p represents a prediction horizon, $r(t+i)$ is a prescribed target value of MAP control on time point $t+i$, and $\Delta MAP_{NN}(t+i)$ is the predicted MAP output by the NN. The future value of $\Delta MAP_{NN}(t+i)$ can be estimated by the $\Delta MAP_{NN}(t)$ acquired from the backpropagation algorithm [Fig. 4(a) and (b)]. $J(t)$ contained the predicted output after N_p steps to suppress sudden changes in NE infusion rate. The optimal value, $N_p = 3$, was obtained from a simulation using the ΔMAP_{mod}. A predicted response is also shown in Fig. 4(a) for $N_p = 3$. The cost function, $J(t)$, was minimized by a downhill Simplex method for a quadratic function (see Simplex Method for Quadratic Function under Appendix[16,30]).

Combined Control of APC_{NN} and PID ($APC_{NN\text{-}PID}$)

A NN can have many degrees of freedom to allow the learning of nonlinear time-varying characteristics of a patient, which, in turn, precludes the simultaneous optimization of stability and performance speed for the APC_{NN}.[1,14] Because emphasis is given to stability rather than speed in the algorithm's performance, the speed of MAP control was sacrificed to some extent. To supplement the speed performance, we constructed an APC_{NN} combined with a PID control. The PID algorithm in the $APC_{NN\text{-}PID}$ operates when the absolute error between observed MAP and a target value exceeds 10 mmHg [Fig. 2(c)]. Even when the PID control is operating, the NN continues learning the characteristics of a patient. The $APC_{NN\text{-}PID}$ used the same PID algorithm, NN learning rule, and cost function as those described in the Methods section under PID Control and Adaptive Predictive Control Based on a NN(APC_{NN}).

PID Control Based on Fuzzy Inference

Fuzzy inference[5] is the process of formulating and mapping from a given input to an output using fuzzy logic.[12,35] To adjust the proportional gain (K_P) of the PID controller

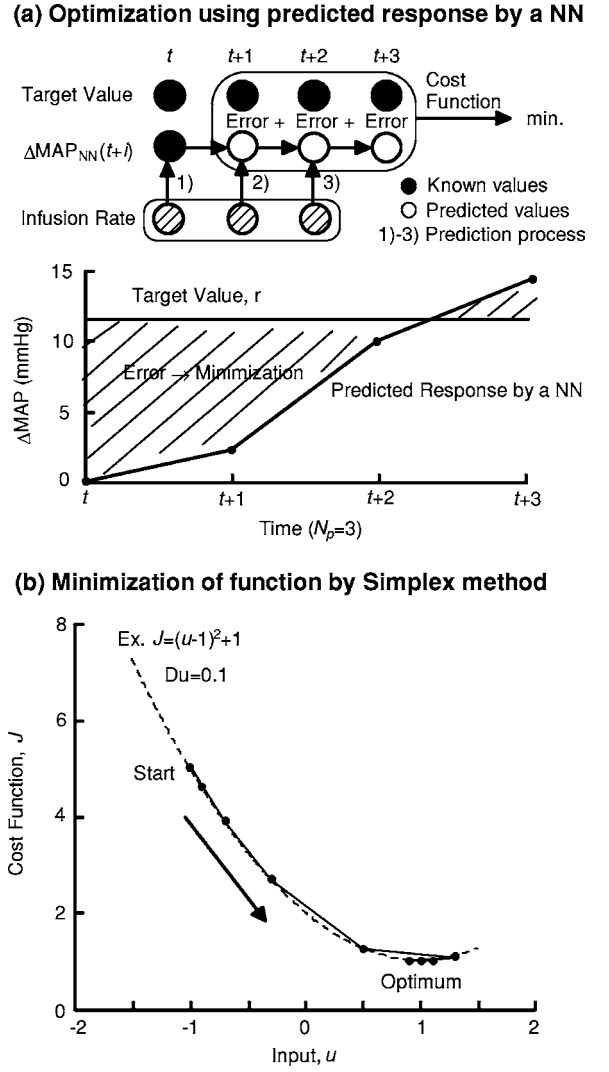

FIGURE 4. (a) Optimization of infusion rate using predicted response by a NN. (b) An example of minimization of a cost function by the downhill Simplex method for a quadratic function.

during the MAP control, a fuzzy inference system was used [Fig. 2(d)]. The basic structure for the adjustment of K_P is shown in Fig. 5. The inputs to the fuzzy inference system are the positive change from target value to $\Delta MAP(t)$ (overshoot, mmHg) and the difference between $\Delta MAP(t-1)$ and $\Delta MAP(t)$ (slope, mmHg 10 s^{-1}), and the output is the proportional gain, K_P, on the PID controller. The fuzzy inference process (Fig. 5) can be described as follows.

Step 1. Fuzzify Inputs. The first step is to take the inputs and determine the degree belonging to each of the appropriate fuzzy sets via membership functions (curves defining how each point in the input space is mapped to a degree of a membership function). In the present study, the triangular membership function formed by straight lines was used. The adjustment of K_P is built on three rules:

Rule 1. IF overshoot is small or slope is small THEN K_P is large.
Rule 2. IF overshoot is middle or slope is middle THEN K_P is middle.
Rule 3. IF overshoot is large or slope is large THEN K_P is small.

Each of the rules depends upon resolving the inputs into a number of different fuzzy linguistic sets: "overshoot is small," "slope is large," etc. The inputs must be fuzzified according to each of these linguistic sets. Step 1 in Fig. 5 shows how large the overshoot (rated on a scale of 5 to 15) or the slope (rated on a scale of 5 to 15) is via its membership functions [0, 1]. For example, when an overshoot of 8 (given our graphical definition of "overshoot is small") is selected, the degree of membership function corresponds to $\mu = 0.4$ for the "small" membership function. In this manner, each input is fuzzified over all the qualifying membership functions required by the rules.

Step 2. Apply Fuzzy Operator. The inputs to the fuzzy operator are two membership values from fuzzified input variables in Step 1, and the output is a single value. To determine the single output as the membership value, the OR operator was used in the present study[12]:

$$\mu_C = \max . \{\mu_A(x_1), \mu_B(x_2)\} \tag{8}$$

where $\mu_{(\cdot)}$ is the degree of the membership function. A and B are fuzzy sets in overshoot and slope and serve as inputs to the antecedent of the fuzzy rules. C is a fuzzy set in the values selected as the input to the consequent of the rules. The $x_{(\cdot)}$ is the input to the membership function. For example, when the antecedent of rule 1 is evaluated, two different pieces of the antecedent ("overshoot is small" and "slope is small") yield the fuzzy membership values 0.4 and 0, respectively. In this case, the OR operator selects the maximum of the two values, 0.4.

Step 3. Apply Implication Method. A consequent (K_P, a scale of 0.05–0.25) of the three rules is a fuzzy set represented by a membership function [0, 1] weighting appropriately the linguistic characteristics that are attributed to it. The consequent is reshaped using a function associated with the antecedent in order to determine a single number. The input for the implication process is a single number given by the antecedent, and the output is a fuzzy set. In the present study, an implication method was used by the AND operator[12]:

$$\mu_E(x_{3i}) = \min . \{\mu_C(x_{3i}), \mu_D(x_{3i})\} \quad i = 0, 1, \ldots, 20 \tag{9}$$

where C contains the values determined by Step 1. D is a fuzzy set in K_P for the antecedent of fuzzy rules. E is a fuzzy set in the values selected for the aggregation procedure (Step 4). The input range of $x_{(\cdot)}$ was divided by 20 to discretize the time domain. The AND operator selects the minimum of the two values as a single number given by the

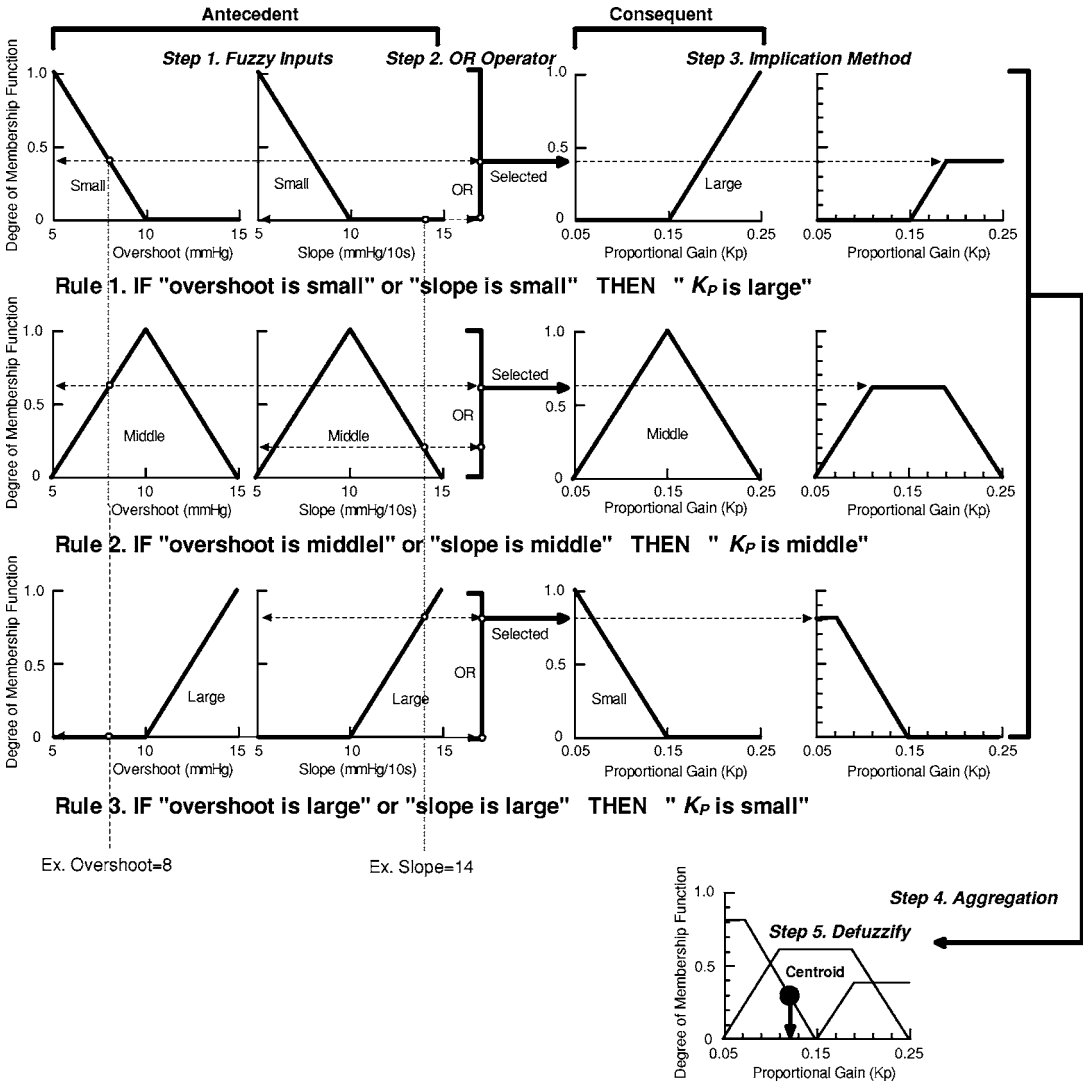

FIGURE 5. An example of a fuzzy inference system. The process for fuzzy inference is shown as Steps 1 to 5. The proportional gain (K_p) in the improved PID control was updated through the process for the fuzzy inference.

antecedent and the membership function of the consequent (Step 3 in Fig. 5).

Step 4. Aggregate All Outputs. Aggregation is the process by which the fuzzy sets that represent the outputs of each rule are combined into a single fuzzy set. Aggregation only occurs once for each output variable, just prior to the fifth and final step, defuzzification. The input of the aggregation process is the list of truncated output functions returned by the implication process for each rule. The output of the aggregation process is one fuzzy set for each output variable. The aggregation was performed by the selection of the maximum of two values in the membership functions[12]:

$$\mu_F(x_{3i}) = \max.\{\mu_{E1}(x_{3i}), \mu_{E2}(x_{3i}), \mu_{E3}(x_{3i})\}$$
$$i = 0, 1, \ldots, 20 \tag{10}$$

where $E1$, $E2$, and $E3$ are the fuzzy sets determined by the Steps 1 to 4 under the rules 1, 2, and 3, respectively. F is a fuzzy set acquired from the result of the aggregation process. In Fig. 5, all three rules have been placed together to show how the output of each rule is combined, or aggregated, into a single fuzzy set whose membership function assigns a weighting for every output (K_P) value.

Step 5. Defuzzify. Because the aggregate of a fuzzy set encompasses a range of output values, it must be defuzzified in order to resolve a single output value from the set. The centroid calculation (center of gravity of the resulting curve) is used to determine the action that the controller will actually take. In the present study, the proportional gain for update, K_P^*, was calculated as follows[35]:

$$K_P^* = \frac{\sum_{i=0}^{20} \mu_F(x_{3i}) \cdot x_{3i}}{\sum_{i=1}^{20} \mu_F(x_{3i})} \tag{11}$$

Model Predictive Control (MPC)

Figure 2(e) shows the diagram of the MPC. The drug infusion rate is computed to minimize the cost function [$P(t)$]:

$$P(t) = \sum_{i=1}^{N_p} [r(t+i) - \Delta\mathrm{MAP}_{\mathrm{mod}}(t+i)]^2 \qquad (12)$$

where N_p is a prediction horizon, $r(t+i)$ is a prescribed target value of MAP control on time point $t+i$, and $\Delta\mathrm{MAP}_{\mathrm{mod}}(t+i)$ is a model predicted output on time point $t+i$. $N_p = 3$ was used in the present study.

To calculate the future output, $\Delta\mathrm{MAP}_{\mathrm{mod}}(t+i)$, in the cost function, $P(t)$, we used the discrete linear step response model using the $\Delta\mathrm{MAP}_{\mathrm{mod}}(t)$ described in Methods under Modeling of MAP Response. The predicted output at the ith future point is shown as follows:

$$\Delta\mathrm{MAP}_{\mathrm{mod}}(t+i) = \sum_{\tau=0}^{i} g(\tau)\cdot\Delta T\cdot u(t+i-\tau) + \sum_{\tau=i+1}^{N_m} g(\tau)\cdot\Delta T\cdot u(t-\tau) + d(t) \qquad (13)$$

where $u(\cdot)$ is the infusion rate of NE (μg kg^{-1} min^{-1}) and $g(\cdot)$ is the unit impulse response (mmHg) which is consistent with that in Fig. 1(b). ΔT is the sampling interval (s) and N_m is the finite number of terms in the model of the unit impulse response. The parameters of $\Delta\mathrm{MAP}_{\mathrm{mod}}$ where $\Delta T = 10$ and $N_m = 30$ [Eq. (13)] includes 1) the present and all future moves of the manipulated variables that were used to solve the cost function, $P(t)$, 2) the past values of the manipulated variables (completely known at time t), and 3) the predicted disturbance calculated as the difference between the current measurements and output from the predicted model [$d(t) = \mathrm{MAP}_{\mathrm{mod}}(t) -$ actual MAP(t)] at the tth sampling time. The $d(t)$ represents model mismatch and unmodeled disturbances that enter the system at time t, and is assumed to be constant over the prediction horizon due to lack of an explicit means of predicting the mismatch or disturbance.[22]

Simulation Study

Protocol 1

We simulated MAP control using the $\Delta\mathrm{MAP}_{\mathrm{mod}}$ against acute hypotension. The exogenous pressure perturbation was introduced at a constant speed of -18 mmHg min^{-1} for 2 min, and then maintained at -36 mmHg for 5 min. Random noise within ± 1 mmHg was added to $\Delta\mathrm{MAP}_{\mathrm{mod}}$ and acute hypotension to mimic physiological variation. The target value of MAP control was set at the baseline MAP, i.e., $\Delta\mathrm{MAP} = 0$. The sampling interval was 10 s and each controller described below updated the NE infusion rate every 10 s. The NE infusion rate [$u(t)$) was bounded by $0 \le u(t) \le 6$ μg kg^{-1} min^{-1}]. The controllers used were the conventional PID controller, $\mathrm{APC_{NN}}$, and $\mathrm{APC_{NN\text{-}PID}}$. To see how the NN parameters changed as a function of time, the weights in the NN were recorded during $\mathrm{APC_{NN}}$ in the simulation study.

Protocol 2

To study the robustness to the MAP change to the drug, we simulated MAP control using the $\Delta\mathrm{MAP}_{\mathrm{mod}}$ [Fig. 1(b)], which was twice as large as the $\Delta\mathrm{MAP}_{\mathrm{mod}}$ response against acute hypotension. Because each controller was designed to optimize the controller performance under the assumption of the $\Delta\mathrm{MAP}_{\mathrm{mod}}$ response [Fig. 1(b)], the twice $\Delta\mathrm{MAP}_{\mathrm{mod}}$ response was unknown to all controllers. Random noise within ± 1 mmHg was added to $\Delta\mathrm{MAP}_{\mathrm{mod}}$. An exogenous pressure perturbation was introduced at a constant speed of -18 mmHg min^{-1} for 2 min, and then maintained at -36 mmHg for 5 min. The target value of MAP control was set at the baseline MAP. The sampling interval was 10 s and each controller updated the infusion rate of NE every 10 s. The infusion rate of NE [$u(t)$] was bounded by $0 \le u(t) \le 6$ μg kg^{-1} min^{-1}.

The controllers used were the conventional PID controller, $\mathrm{APC_{NN}}$, and $\mathrm{APC_{NN\text{-}PID}}$. In addition, to increase robustness during the MAP control, we tested PID control based on fuzzy inference for adjusting the proportional gain, K_P, during the closed-loop control. MPC was also tested in order to examine the performance of the simple predictive control compared with $\mathrm{APC_{NN}}$ or $\mathrm{APC_{NN\text{-}PID}}$.

Animal Study

The animal study conformed to the *Guide for the Care and Use of Laboratory Animals published by the US National Institutes of Health* (NIH Publication No. 85-23, revised 1996). The parameter values used in the simulation were also used in the animal study.

Surgical Preparations

Twelve Japanese white rabbits weighing 2.4–2.7 kg were anesthetized via intravenous injection (2 ml kg^{-1}) with a mixture of urethane (250 mg ml^{-1}) and α-chloralose (40 mg ml^{-1}). The rabbits were ventilated artificially with oxygen-enriched room air. To maintain the appropriate level of anesthesia, supplemental doses of the anesthetics were administered continuously (0.2–0.5 ml kg^{-1} h^{-1}, i.v.). MAP was measured using a high-fidelity pressure transducer (Millar Instruments, Houston, TX, USA) inserted into the right femoral artery. A catheter was introduced into the left femoral artery. A computer-controlled infusion pump (CFV-3200; Nihon Kohden, Tokyo, Japan) was attached to the arterial line for later arterial blood withdrawal and re-infusion. A double-lumen catheter was introduced into

the right femoral vein for administration of anesthetic agent and NE. Another computer-controlled infusion pump was used for NE infusion. The NE infusion rate was controlled through a 12-bit digital-to-analog converter connected to a laboratory computer. Body temperature was maintained at around 38°C with a heating pad throughout the experiment.

Protocols

To test the robustness of each control system, we used two different concentrations of NE. In Protocol 1 ($n = 6$), we used a NE solution of 25 μg ml^{-1}. In Protocol 2 ($n = 6$), which was performed in another group of rabbits, we used a NE solution of 50 μg ml^{-1}. In both Protocols 1 and 2, we first determined the volume of blood withdrawal necessary to induce a MAP fall of approximately 40 mmHg. The speed of blood withdrawal was calculated so that the hemorrhage was completed in 2 min. The average speed of blood withdrawal was 18.2 ± 6.8 ml min^{-1} in Protocol 1 and 20.2 ± 7.5 ml min^{-1} in Protocol 2.

In each hemorrhage trial, we recorded baseline MAP for 1 min prior to the hemorrhage and used the average baseline MAP as a target value. The arterial blood was then withdrawn at a predefined constant speed for 2 min to induce hemorrhage. Thereafter the hemorrhaged state was maintained for 5 min, rendering a total hemorrhage period of 7 min. We measured changes in MAP during hemorrhage under the uncontrolled condition, PID control, APC_{NN}, and $APC_{NN\text{-}PID}$. After 7 min of hemorrhage, the blood was slowly re-infused. We performed four trials (randomly ordered), in each rabbit, with a washout period of 20 min. Instantaneous MAP data was sampled continuously through a 12-bit analog-to-digital converter at 10 Hz and the MAP data (averaged every 10 s) was used as the system controlled variable.

Data Analysis

The performance of each controller was compared using several indices: maximum MAP fall during the initial 2 min of the hemorrhage (maximum fall), maximum absolute error between a target and observed MAP value calculated from the last 2 min of hemorrhage period (maximum error), and average absolute value of error between a target and observed MAP value over the entire hemorrhage period (average error). The elapsed time for MAP that first reached the target value within -5 mmHg (recovery time) was also calculated.

Statistical Analysis

All data were presented as mean $\pm$ SD. The differences of the performance indices among controllers were examined by one-way analysis of variance with repeated measures and the Bonferroni *post hoc* test.[7] Statistical significance was assigned to differences producing $p < 0.05$.

RESULTS

Simulation Study

Protocol 1

Figure 6 shows the simulation results from using (a) PID ($K_P = 0.3$, $T_I = 20$, and $T_D = 5$) control, (b) APC_{NN} ($K_n = 0.2$, and $N_p = 3$), and (c) $APC_{NN\text{-}PID}$ ($K_n = 0.2$, $N_p = 3$, $K_P = 0.3$, $T_I = 20$, and $T_D = 5$). Changes in MAP (left panels) and the NE infusion rate (right panels) are presented. The fall of MAP was -36 mmHg in 2 min and the hypotension continued for 5 min. In Fig. 6(a), (b), and (c), thick lines are MAP responses and thin lines are the uncontrolled condition. Dotted lines in Fig. 6(b) and (c) represent MAP responses predicted by the NN. When the controllers were activated, MAP returned to the target value. PID control with fixed parameters provided a quick and stable MAP regulation in the present simulation [Fig. 6(a), left]. APC_{NN} showed a maximum MAP fall greater than that of PID control [Fig. 6(b), left]. The recovery time was longer using APC_{NN} compared to PID control. The elevation in NE infusion rate was slow in APC_{NN} [Fig. 6(b), right]. $APC_{NN\text{-}PID}$ achieved MAP recovery faster than APC_{NN} [Fig. 6(c), left]. The PID component of the $APC_{NN\text{-}PID}$ system operated from 30 to 60 s when the MAP fall exceeded 10 mmHg.

Figure 7 shows the time series of the weights in the NN during the simulation study of APC_{NN} in the Protocol 1. Dotted lines in Fig. 7 represent the weights as bias. During the initial hypotension for 120 s, the weights as bias in the output layer [Fig. 7(c)] were dramatically decreased compared to the other weights, which were only slightly changed. Because the bias absorbed the offset of the acute hypotension, they would have kept the trained response characteristics to the infusion rate of NE in the NN. Therefore, it appears fine adjustments of the difference between the actual and NN-predicted MAP response were performed by modifications to the other weights in the NN.

Protocol 2

Figure 8 shows the simulation results of (a) PID ($K_P = 0.3$, $T_I = 20$, and $T_D = 5$) control, (b) APC_{NN} ($K_n = 0.2$ and $N_p = 3$), and (c) $APC_{NN\text{-}PID}$ ($K_n = 0.2$, $N_p = 3$, $K_P = 0.3$, $T_I = 20$, and $T_D = 5$) during the unexpected MAP change to NE, *i.e.* the magnitude of MAP change to NE was doubled. Changes in MAP (left panels) and the NE infusion rate (right panels) are presented. In Fig. 8(a), (b), and (c), thick lines are MAP responses and thin lines are the uncontrolled condition. Dotted lines in Fig. 8(b) and (c) represent MAP responses predicted by the NN. The fall of MAP was -36 mmHg in 2 min and

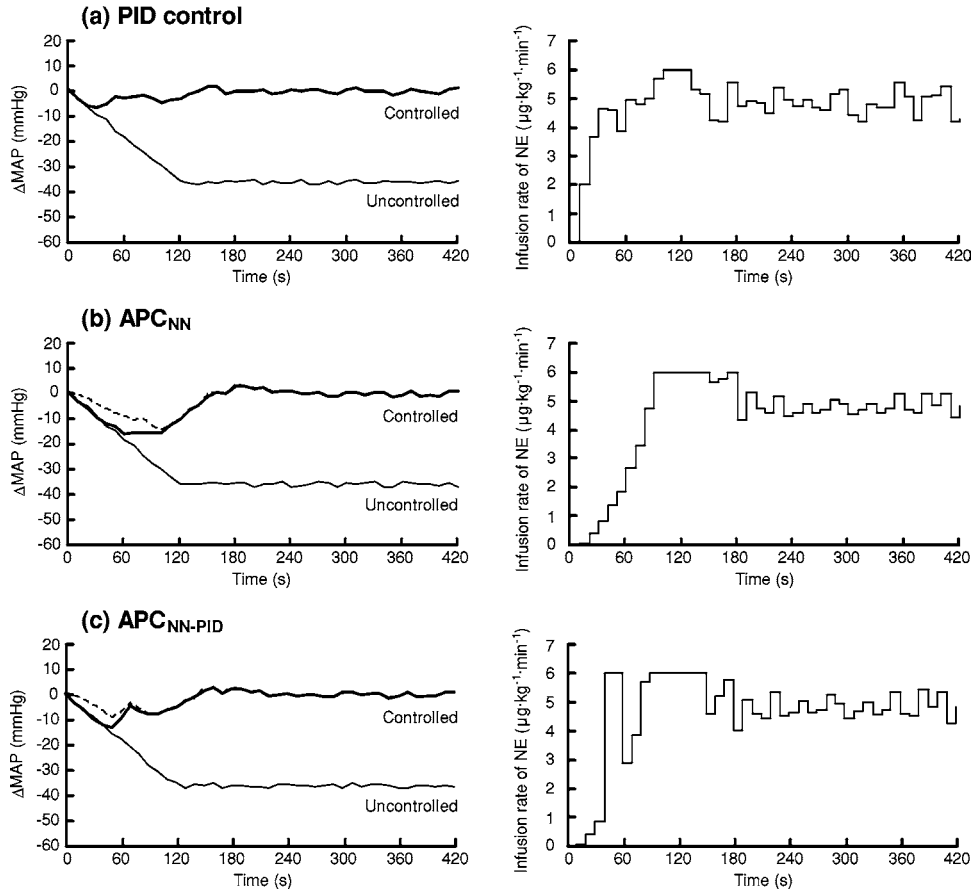

FIGURE 6. Simulation results of (a) PID control, (b) APC$_{NN}$, and (c) APC$_{NN\text{-}PID}$. The left panels show the MAP responses (thick solid line) and the uncontrolled condition (thin solid line). Dotted lines in (b) and (c) represent MAP responses predicted by the NN. The right panels show the NE infusion rate. Acute hypotension of −36 mmHg was completed in 2 min and maintained thereafter.

the hypotension continued for 5 min. Under PID control, although MAP returned to the target value within approximately 40 s, sustained MAP oscillation within ±10 mmHg occurred thereafter [Fig. 8(a), left]. The NE infusion rate cycled between 0 and the predefined maximum value. Under APC$_{NN}$, MAP decreased to −10 mmHg at 60 s, returned to the target value within approximately 120 s, exceeded the target value by approximately 10 mmHg at 150 s, and again returned to the target value at approximately 200 s [Fig. 8(b), left]. Under APC$_{NN\text{-}PID}$, MAP returned to the target value within approximately 70 s, exceeded the target value by approximately 10 mmHg at 100 s, and again returned to the target value at approximately 200 s [Fig. 8(c), left].

Figure 8(d) and (e) shows the simulation results of (d) improved PID control (initial parameters: $K_P = 0.3$, $T_I = 20$, and $T_D = 5$), and (e) MPC ($N_p = 3$) during the unexpected MAP change. Using improved PID control, MAP returned to the target value within approximately 60 s but had a slight oscillation within ±5mmHg (Fig. 8(d), left). The K_P was changed from 0.3 as the initial value to 0.187 at 40 s (slope > 5) and 0.193 at 50 s (actual ΔMAP > 5). Under MPC, although MAP returned to the target value within approximately 40 s, sustained MAP oscillation within ±10 mmHg occurred thereafter [Fig. 8(e), left]. The NE infusion rate cycled between 0 and 6 under the unexpected MAP change.

Animal Study

Protocol 1

Figure 9 shows typical examples of (a) PID ($K_P = 0.3$, $T_I = 20$, and $T_D = 5$) control, (b) APC$_{NN}$ ($K_n = 0.2$ and $N_p = 3$), and (c) APC$_{NN\text{-}PID}$ ($K_n = 0.2$, $N_p = 3$, $K_P = 0.3$, $T_I = 20$, and $T_D = 5$) obtained from one animal in Protocol 1. In Fig. 9(a), (b), and (c), thick lines are MAP responses and thin lines are the uncontrolled condition. Dotted lines in Fig. 9(b) and (c) represent MAP responses predicted by the NN. Under PID control, although MAP returned to the target value within approximately 60 s, four of six animals showed MAP oscillation within ±10 mmHg [Fig. 9(a), left]. Under APC$_{NN}$, MAP returned to the target value within approximately 120 s, exceeded the target value by approximately 5 mmHg at 150 s, and again returned

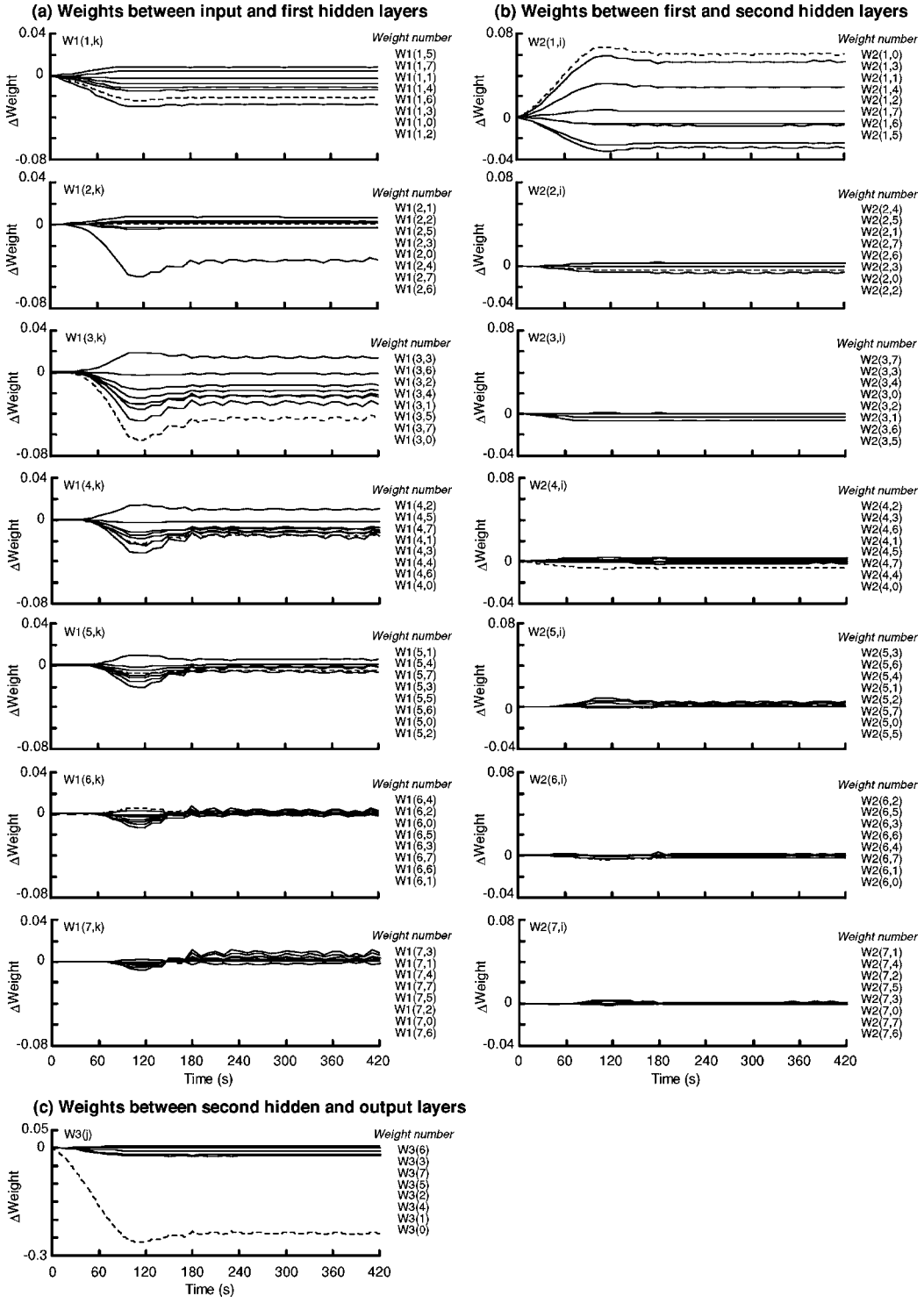

FIGURE 7. Time course of weight change from the weight at the starting time in the NN (Δweight) during the simulation study of APC_{NN} in Fig. 6 (b). (a) Weights between input and first hidden layers, (b) Weights between first and second hidden layers, and (c) Weights between second hidden and output layers. Weight numbers (*W*1(*i*, *k*), *W*2(*j*, *i*), and *W*3(*j*)) in the Figure correspond to those in Fig. 3. Each weight number was ordered from a high to low weight value at the final time. Dotted lines represent the weights as bias.

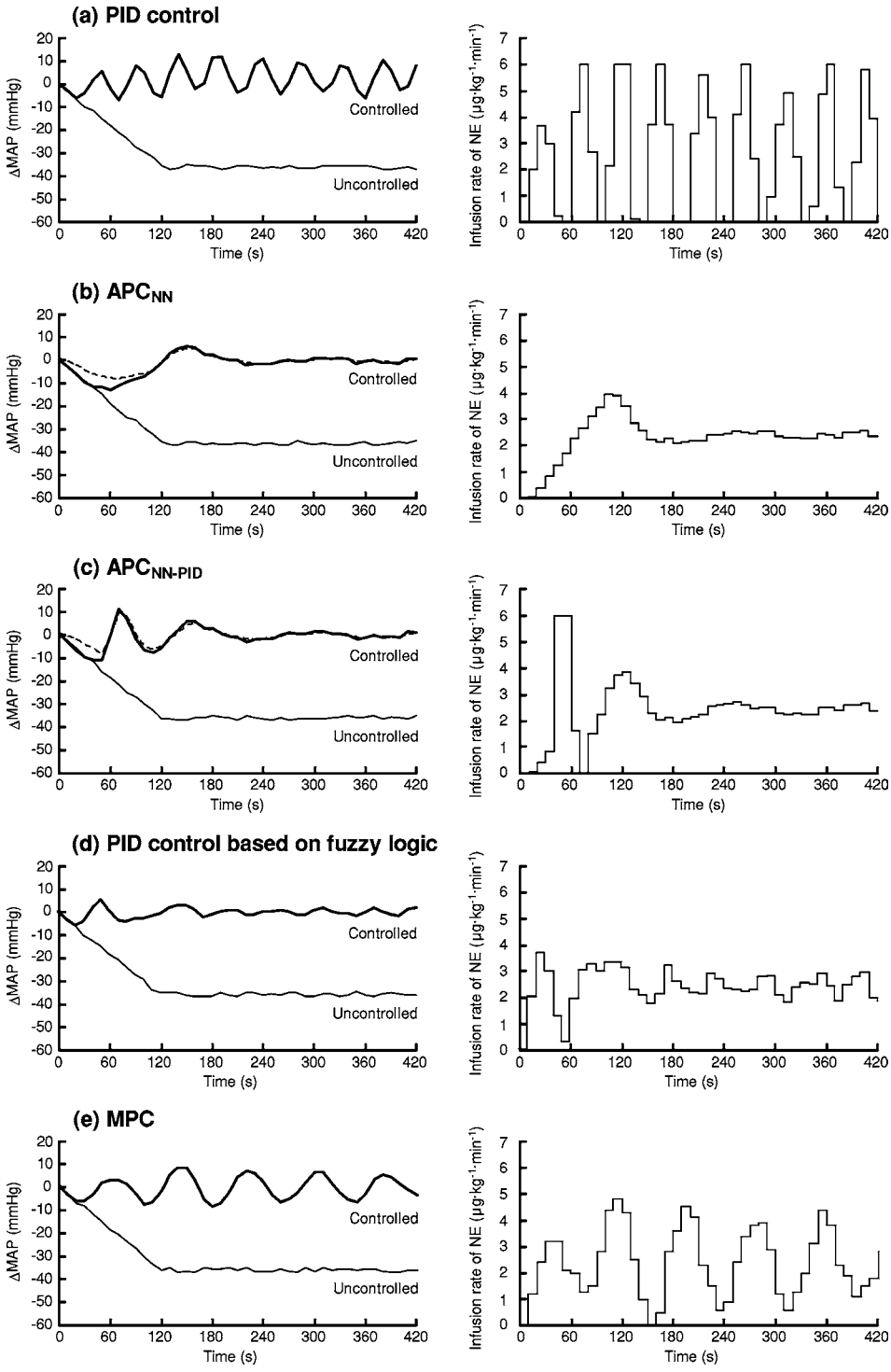

FIGURE 8. The simulation results of (a) PID control, (b) APC$_{NN}$, (c) APC$_{NN-PID}$, (d) PID control based on fuzzy inference, and (e) MPC under the unexpected MAP change. Left panels are changes in MAP and right panels are the NE infusion rate. Dotted lines in (b) and (c) represent MAP responses predicted by the NN.

to the target value at approximately 200 s [Fig. 9(b), left]. Under APC$_{NN-PID}$, MAP returned to the target value within approximately 60 s, exceeded the target value by approximately 8 mmHg at 150 s, and again returned to the target value at approximately 200 s [Fig. 9(c), left].

Figure 10 summarizes the performance indices obtained from Protocol 1. All controllers significantly attenuated the maximum MAP fall. The maximum MAP fall was greater in APC$_{NN}$ than in PID control. Neither maximum error nor average error differed among the three controllers. The

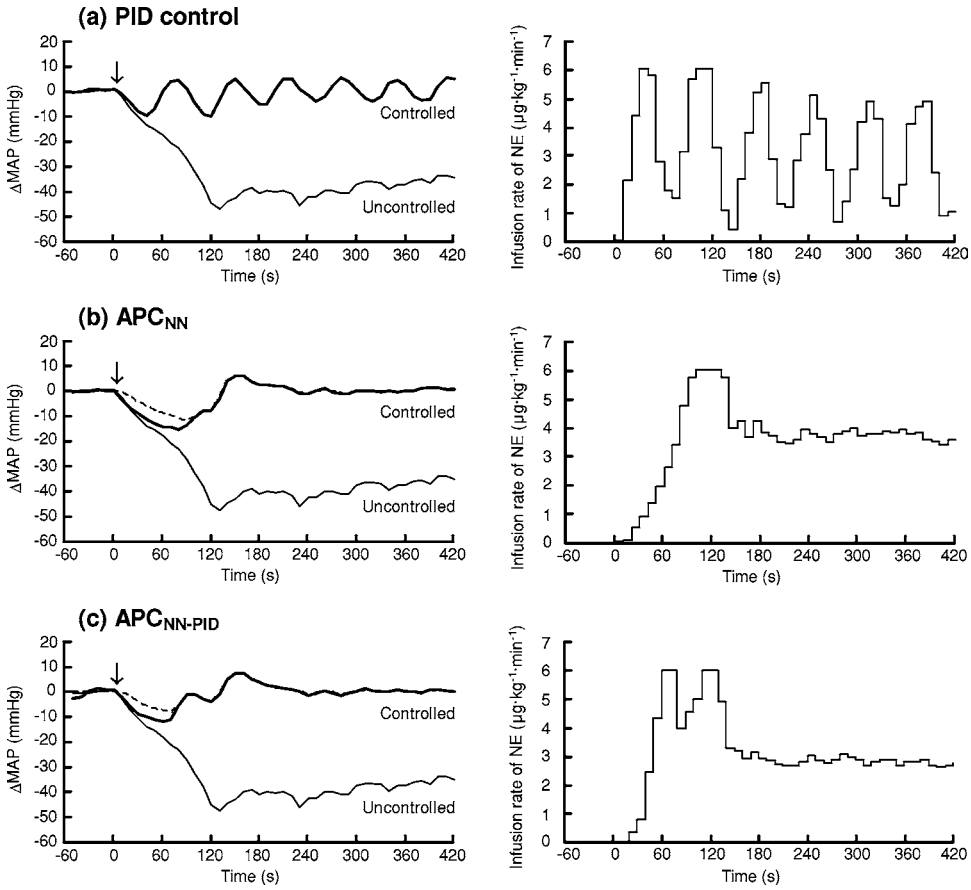

FIGURE 9. Typical examples of (a) PID control, (b) APC$_{NN}$, and (c) APC$_{NN-PID}$ obtained from one animal in Protocol 1. The left panels show the MAP responses (thick solid line) and the uncontrolled condition (thin solid line). Dotted lines in (b) and (c) represent MAP responses predicted by the NN. Arrows indicate the start point of hemorrhage and MAP control. The right panels show the NE infusion rate.

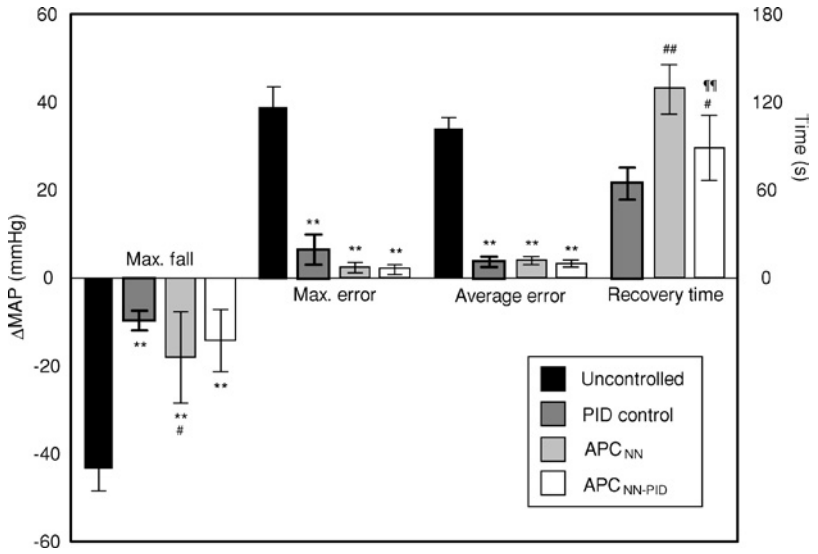

FIGURE 10. Maximum fall, maximum error, average absolute value of error between the target and observed MAP value (average error), and recovery time in the uncontrolled condition, PID control, APC$_{NN}$, and APC$_{NN-PID}$ obtained from Protocol 1. $^{**}P < 0.01$ vs. the uncontrolled condition. $^{\#\#}P < 0.01$ vs. PID control. $^{\#}P < 0.05$ vs. PID control. ¶¶$P < 0.01$ vs. APC$_{NN}$.

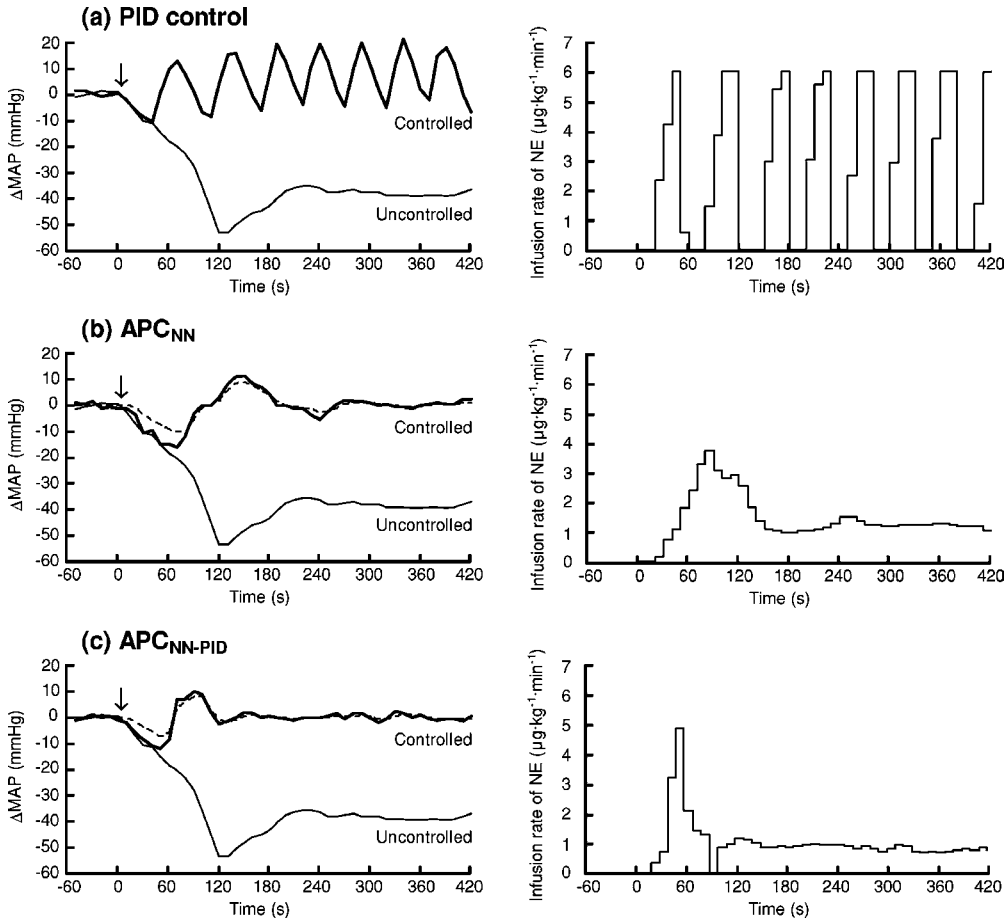

FIGURE 11. Typical examples of (a) PID control, (b) APC_{NN}, and (c) APC_{NN-PID} obtained from one animal in Protocol 2. The left panels show the MAP responses (thick solid line) and the uncontrolled condition (thin solid line). Dotted lines in (b) and (c) represent MAP responses predicted by the NN. Arrows indicate the start point of hemorrhage and MAP control. The right panels show the NE infusion rate.

recovery time was significantly shorter in PID control than in APC_{NN} and APC_{NN-PID}. The recovery time was significantly shorter in APC_{NN-PID} than in APC_{NN}. The average blood loss was 14.1 ± 4.7 ml kg^{-1} body weight. The average MAP was decreased from 107.7 ± 9.1 to 73.9 ± 10.2 mmHg at 2 min of hemorrhage under the uncontrolled condition.

Protocol 2

Figure 11 shows typical examples of (a) PID (K_P = 0.3, T_I = 20, and T_D = 5) control, (b) APC_{NN} (K_n = 0.2 and N_p = 3), and (c) APC_{NN-PID} (K_n = 0.2, N_p = 3, K_P = 0.3, T_I = 20, and T_D = 5) in Protocol 2. In Fig. 11(a), (b), and (c), thick lines are MAP responses and thin lines are the uncontrolled condition. Dotted lines in Fig. 11(b) and (c) represent MAP responses predicted by the NN. Under PID control, although MAP returned to the target value within approximately 40 s, sustained MAP oscillation occurred thereafter in all six animals. In these animals MAP exceed the target value by 20 mmHg [Fig. 11(a), left]. The NE infusion rate cycled between 0 and the predefined maximum value. Under APC_{NN}, MAP returned to the target value within approximately 120 s, exceeded the target value by approximately 10 mmHg at 150 s, decreased by approximately 5 mmHg at 240 s, and again reached the target value at approximately 300 s [Fig. 11(b), left]. Under APC_{NN-PID}, MAP returned to the target value within approximately 70 s, exceeded the target value by approximately 10 mmHg at 100 s, and again reached the target value at approximately 120 s [Fig. 11(c), left].

Figure 12 summarizes the performance indices obtained from Protocol 2. All controllers significantly attenuated the maximum MAP fall. There were no significant differences in the maximum MAP fall among the three controllers. Both maximum error and average error were significantly smaller in APC_{NN} and APC_{NN-PID} than in PID control. The recovery time was significantly shorter in PID control than in APC_{NN} and APC_{NN-PID}. The recovery time in APC_{NN-PID} was significantly shorter than in APC_{NN}. The average blood loss was 15.5 ± 5.4 ml kg^{-1} body weight. The average

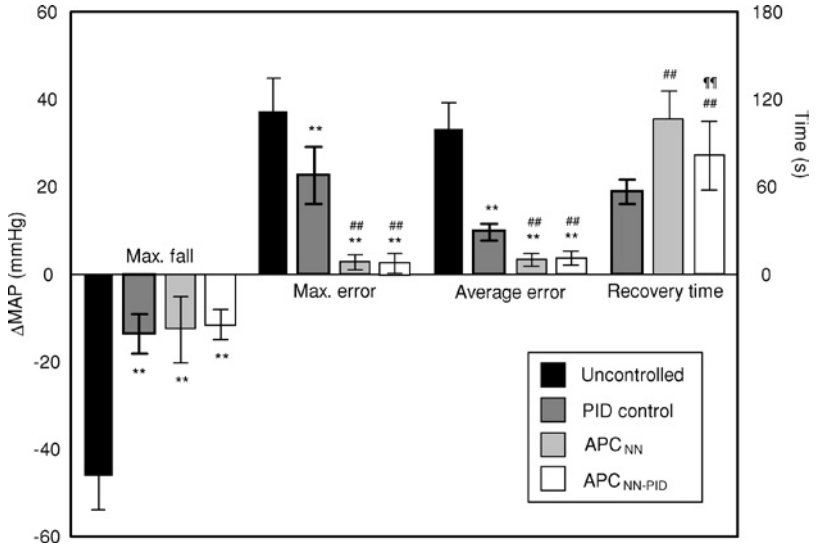

FIGURE 12. Maximum fall, maximum error, average error, and recovery time in the uncontrolled condition, PID control, APC_{NN}, and $APC_{NN\text{-}PID}$ obtained from Protocol 2. $^{**}P < 0.01$ vs. the uncontrolled condition. $^{\#\#}P < 0.01$ vs. PID control. $\P\P P < 0.01$ vs. APC_{NN}.

MAP decreased from 101.4 ± 9.9 to 68.4 ± 9.4 mmHg at 2 min of hemorrhage under the uncontrolled condition.

DISCUSSION

Prolonged hypotension below 45 mmHg could cause circulatory insufficiency in vital organs resulting in death.[8] The arterial baroreflex is an important negative feedback mechanism that maintains MAP at normal operating pressure against any pressure disturbance. In the present study, however, the average MAP fall exceeded −30 mmHg under the uncontrolled condition (Figs. 9 and 11). This is to say that the buffering effect of the arterial baroreflex was not sufficiently strong to prevent acute and severe hypotension despite the fact that the sympathetic system appears to have been maximally activated through the baroreflex negative feedback. All systems tested were able to prevent severe hypotension by controlling the infusion of NE, which acted on the heart, capacitance vessels, and resistance vessels to increase MAP. There might be a considerable reserve in the circulatory responses to NE even when the sympathetic system is fully activated through the baroreceptor unloading. Rapid action and the short half-life (approximately 2 min) of NE were convenient for MAP control using the automated drug infusion systems.

Although PID control did not show MAP oscillation in the simulation study [Fig. 6(a)], MAP oscillation within ±10 mmHg occurred in four of the six animals in Protocol 1 of the animal study [Fig. 9(a)]. Because PID parameters were tuned beforehand using a model of MAP response and fixed during the control periods, PID control could not optimize the MAP control with respect to individual animals. In Protocol 2 of the animal study, PID control failed to stabilize MAP in all animals [Fig. 11(a)]. A large MAP oscillation was sustained until the study was terminated at 7 min. These results suggest that using the PID control could endanger patients in clinical settings if the PID parameters are not individualized, which is unrealistic because the MAP response to NE infusion, in each subject, is unknown beforehand.

In the modeling of MAP response to NE, we used an average step response of 5 min during NE infusion in anesthetized rabbits without hemorrhage. If fine tuning of a PID controller is performed based on the pathological model of acute hypotension, the result of PID control in the animal study might have been better compared to the results from the present study. However, the modeling of MAP response to a therapeutic agent in acute hypotension is actually quite difficult due to the complex pharmacological variability and the various reactions to bleeding.

In contrast to PID control, the NN in APC_{NN} and $APC_{NN\text{-}PID}$ systems offer the ability to adapt to MAP changes based upon an individual's measurements, in real time, and learn the MAP response to NE infusion in respective animals. In Protocol 1 of the animal study, because hemorrhage itself was not predictable by the NN, ΔMAP predicted by the NN differed from measured ΔMAP in the initial phase of blood withdrawal [Fig. 9(b) and (c)]. However, ΔMAP predicted by the NN approximated the measured ΔMAP within 2 min, suggesting that the NN had learned the information required to control MAP. Thereafter, the MAP was stabilized at the target value in both APC_{NN} and $APC_{NN\text{-}PID}$. In Protocol 2 of the animal study, despite the use of a higher NE concentration, both APC_{NN} and $APC_{NN\text{-}PID}$ could prevent sustained MAP oscillation [Fig. 11(b) and (c)]. The maximum error and average error values in APC_{NN} and $APC_{NN\text{-}PID}$ were similar between Protocols 1 and 2 of the animal study, suggesting that the

control performance was not influenced by NE concentration. In other words, APC_{NN} and $APC_{NN\text{-}PID}$ might be able to adjust themselves for optimal MAP control even when the MAP response to NE infusion varied significantly among subjects.

Despite the potential benefit of automated drug infusion systems for MAP control, they have not been widely applied to routine clinical practice. One possible reason might be the difficulty in modeling the nonlinear MAP response to drug infusion.[9] Although various models of MAP response to drug infusion have been developed for MAP control,[22,34] the complexity of these models makes developing a reliable system controller difficult. In the present study, we used a simple first-order delay system as the model of MAP response to NE infusion. The initial connection weights for the NN were determined from the learning results of a linear model, yet APC_{NN} and $APC_{NN\text{-}PID}$ were able to maintain stable MAP regulation in the animal study. The flexibility of a NN coupled with an adaptive control mechanism enabled controlling the nonlinear system even if the controllers were initially designed using a linear model for the controlled system. Because utilization of a NN makes it unnecessary to construct a complex model for MAP response to drug infusion, it seems an ideal tool for designing a system to individualize MAP control in patients.

There are several limitations in the present study. First, to simplify the controller design we used a single control variable, i.e. the NE infusion rate. As the fluid infusion and blood transfusion as well as administration of other drugs are common in clinical practice, a multivariate control is mandatory for any reliable automated drug infusion system. Because a NN can have a multiple-input layer and multiple-output layer,[1] we will be able to extend APC_{NN} and $APC_{NN\text{-}PID}$ to multivariate control systems. Second, because we used a threshold value (± 10 mmHg) to activate PID control in $APC_{NN\text{-}PID}$, NE infusion rate changed discontinuously at $\Delta MAP = \pm 10$ mmHg. Although the discontinuity did not immediately cause the abrupt MAP change by virtue of the velocity form algorithm implemented for PID control, further refinement is required to suppress abrupt changes in the NE infusion rate.

The PID control based on fuzzy inference prevented the MAP response from having oscillations regardless of the unexpected MAP change [Fig. 8(d)]. We think the ideal result was due to the adaptive change of the proportional gain in the PID parameter. As a limitation, the PID controller based on the fuzzy inference has to be programmed with the known or experienced rules fit for the various cases in clinical settings. Because ascertaining all events under clinical circumstances is difficult, the design based on fuzzy rules may require an enormous setup stage. Under MPC, the MAP oscillation within ± 10 mmHg occurred under the unexpected MAP change [Fig. 8(e)] whereas MPC performed fine under the expected MAP change. In the case where the error between the MAP response in MPC and the actual MAP response is large, the cost function containing the weight of inputs or the model bank would be an effective way of adjusting the varying therapeutic sensitivities.[21] If the control conditions are within the expected ranges for the following disturbances; physiological sensitivities to therapeutic agents, interaction between agents, and variances of time dependent changes and nonlinearity; then the improved PID control, the MPC, and the conventional adaptive control will perform well. However, in the clinical setting, the control conditions are dynamic and unexpected patient response may occur. In this case, the model based predictive control or the fuzzy based control alone may not be able to adjust for the physiological changes. Therefore, adding the NN and fuzzy logic to the PID control, APC and MPC will be more effective for unexpected control conditions.

In conclusion, PID control, APC_{NN}, and $APC_{NN\text{-}PID}$ significantly prevented acute and severe hypotension induced by hemorrhage in anesthetized rabbits. Although PID control caused sustained MAP oscillation around the target value, the improved PID control based on fuzzy inference prevented the MAP from having this oscillation. Under the MPC, the MAP oscillation occurred under the unexpected control condition whereas the MPC performed ideally under expected control conditions. Designing a MPC or PID control based on fuzzy inference that is robust, may require an enormous amount of time to accurately model because of intra- and inter-patient variability in response to pharmacological drugs containing nonlinearity, pure time delay changes, and other unforeseen interactions and disturbances.[10,23] Both APC_{NN} and $APC_{NN\text{-}PID}$ showed more stable MAP control compared to PID control regardless of the NE concentration administered. The recovery time of $APC_{NN\text{-}PID}$ was shorter than that of APC_{NN}. Despite the simple design based on the first order delay model with unknown hypotension and drug sensitivity, the controls based on a NN approach were offered a robust control even in the presence of unexpected hypotension and unknown drug sensitivity. Therefore, utilization of a NN for adaptive predictive control would facilitate the development of an automated drug infusion system for quick and stable MAP control. However, further investigations using controls based on a NN will be required.

APPENDIX

Feed-Forward Output Using a NN

Input Layer to First Hidden Layer

The number of units in the first hidden layer of a NN was set to seven (the same number as the input units) using a trial and error approach. First, vector v_0 in the first hidden layer was calculated as follows:

$$v_0(i) = \sum_{k=0}^{7} W1(i,k) \cdot in(k) \quad i = 1, 2, \ldots, 7$$

where $W1(i, k)$ is the weight matrix, and $in(k)$ is the input to the first hidden layer. The inputs contain the unit bias, $in(0) = 1$.

The output of each neuron, $v_0(i)$, was transformed into $v(i)$ through a hyperbolic tangent function:

$$v(i) = \tanh\left(\frac{v_0(i)}{2}\right) = \frac{1 - \exp[-v_0(i)]}{1 + \exp[-v_0(i)]} \quad i = 1, 2, \ldots, 7$$

$v(0) = 1$ is the bias input to the second hidden layer.

First Hidden Layer to Second Hidden Layer

The number of units in the second hidden layer on a NN was set to seven (the same number as the first hidden layer units). $z_0(\cdot)$ was calculated as follows:

$$z_0(i) = \sum_{i=0}^{7} W2(j, i) \cdot v(i) \quad j = 1, 2, \ldots, 7$$

where $W2(j, i)$ is the weight matrix, and $v(i)$ is the input to the second hidden layer. The inputs contain the unit bias, $v(0) = 1$.

The output of each neuron, $z_0(j)$, was transformed into z(j) through a hyperbolic tangent function:

$$z(j) = \tanh\left(\frac{z_0(j)}{2}\right) = \frac{1 - \exp[-z_0(j)]}{1 + \exp[-z_0(j)]} \quad j = 1, 2, \ldots, 7$$

$z(0) = 1$ is the bias input to the next output layer.

Second Hidden Layer to Output Layer

$\Delta\text{MAP}_{\text{NN}}$ in the output layer was calculated as follows:

$$\Delta\text{MAP}_{\text{NN}}(t) = \sum_{j=0}^{7} W3(j) \cdot z(j)$$

where $W3(j)$ is the weight matrix, and $z(j)$ is the input to the output layer. The inputs contain the unit bias, $z(0) = 1$.

Backpropagation Algorithm for Learning

The modification of weights in each layer on the NN can be described as follows.

Output Layer-Second Hidden Layer

$W3^*(j)$ is the weight matrix after update:

$$W3^*(j) = W3(j) - Kn \cdot \varepsilon \cdot \frac{\partial\text{MAP}_{\text{NN}}}{\partial W3(j)} \quad j = 0, 1, \ldots, 7$$

where

$$\frac{\partial\text{MAP}_{\text{NN}}}{\partial W3(j)} = z(j)$$

$z(j)$ is the input to output layer, which represents the output of each neuron in a hyperbolic tangent function on the second hidden layer.

Second Hidden Layer to First Hidden Layer

$W2^*(j, i)$ is the weight matrix after update:

$$W2^*(j, i) = W2(j, i) - Kn \cdot \varepsilon \cdot \frac{\partial\text{MAP}_{\text{NN}}}{\partial W2(j, i)}$$
$$j = 0, 1, \ldots, 7 : i = 0, 1, \ldots, 7 : v(0) = 1$$

where

$$\frac{\partial\text{MAP}_{\text{NN}}}{\partial W2(j, i)} = \frac{\partial\text{MAP}_{\text{NN}}}{\partial z(j)} \cdot \frac{\partial z(j)}{\partial z_0(j)} \cdot \frac{\partial z_0(j)}{\partial W2(j, i)}$$
$$= W3(j) \cdot \frac{1 - z(j)^2}{2} \cdot v(i)$$

$v(j)$ is the input to the second hidden layer, which represents the output of each neuron in a hyperbolic tangent function on the first hidden layer.

First Hidden Layer to Input Layer

$W1^*(i, k)$ is the weight matrix after update:

$$W1^*(i, k) = W1(i, k) - Kn \cdot \varepsilon \cdot \frac{\partial\text{MAP}_{\text{NN}}}{\partial W1(i, k)}$$
$$i = 1, 2, \ldots, 7 : k = 0, 1, \ldots, 7 : in(0) = 1$$

where

$$\frac{\partial\text{MAP}_{\text{NN}}}{\partial W1(i, k)} = \left[\sum_{j=1}^{7}\left(\frac{\partial\text{MAP}_{\text{NN}}}{\partial z(j)} \cdot \frac{\partial z(j)}{\partial z_0(j)} \cdot \frac{\partial z_0(j)}{\partial v(i)}\right)\right] \cdot \frac{\partial v(i)}{\partial v_0(i)} \cdot \frac{\partial v_0(i)}{\partial W1(i, k)}$$
$$= \left[\sum_{j=1}^{7}\left(W3(j) \cdot \frac{1 - z(j)^2}{2} \cdot w2(j, i)\right)\right] \cdot \frac{1 - v(i)^2}{2} \cdot in(k)$$

$in(k)$ is the input to the first hidden layer, which represents the past input to the NN.

Simplex Method for Quadratic Function

Figure 4(b) shows an example of the simplex method used to solve the quadratic function. The search starting at $u = -1$ reached the minimum point quickly. The steps of the downhill simplex method can be described as follows.[16,30]

Step 1. Calculate $Jx = J(Ux)$ of input Ux.
Calculate $Jy = J(Uy)$ of input $Uy = Ux + Du$ (initial change in quantity, ex. 0.1).

Step 2. Ja = the small number of Jx or Jy, and Ua = the input of the determined Ja.
The other output is Jb, and the input of Jb is Ub.
IF $Du < V$ (value showing convergence, ex. 0.001) THEN stop the Steps.

Step 3. $Uc = Ua + Du$ (opposite direction of Ub).
Calculate $Jc = J(Uc)$ in input Uc.
IF $Jc < Jb$ THEN go to Step 4, ELSE go to Step 5.

Step 4. $Ud = Uc + Du$ (opposite direction of Ub).
Calculate $Jd = J(Ud)$ of input Ud.
IF $Jd < Jc$ THEN $Du = 2 \cdot Du$, $Jx = Ja$, $Ux = Ua$, $Jy = Jd$, and $Uy = Ud$, ELSE $Jx = Jc$, $Ux = Uc$, $Jy = Ja$, and $Uy = Ua$.
Go to Step 1.

Step 5. Calculate $Du = Du/2$, $Ux = Ua$, $Jx = Ja$, $Uy = (Ua + Ub)/2$, and $Jy = J(Uy)$ of input Uy.
Go to Step 1.

ACKNOWLEDGMENTS

This study was supported by Research Grants for Cardiovascular Diseases (9C-1, 11C-3, 11C-7) from the Ministry of Health and Welfare of Japan, by a Health Sciences Research Grant for Advanced Medical Technology from the Ministry of Health and Welfare of Japan, by Grant-in-Aid for Scientific Research (B-11694337, C-11680862, C-11670730) and Grant-in-Aid for Encouragement of Young Scientists (13770378) from the Ministry of Education, Science, Sports, and Culture of Japan, by Research and Development for Applying Advanced Computational Science and Technology from the Japan Science and Technology Corporation, and by the Program for Promotion of Fundamental Studies in Health Science from the Organization for Pharmaceutical Safety and Research.

REFERENCES

[1]Chen, C. T., W. L. Lin, T. S. Kuo, and C. Y. Wang. Adaptive control of arterial blood pressure with a learning controller based on multilayer neural networks. *IEEE Trans. Biomed. Eng.* 44:601–609, 1997.

[2]Delapasse, J. S., K. Behbehani, K. Tsui, and K. W. Klein. Accommodation of time delay variations in automatic infusion of sodium nitroprusside. *IEEE Trans. Biomed. Eng.* 41:1083–1091, 1994.

[3]Fowler, N. O., and R. Franch. Mechanism of pressor response to l-norepinephrine during hemorrhagic shock. *Circ. Res.* 5:153–156, 1957.

[4]Franklin, G. F., J. D. Powell, and M. L. Workman. Digital Control of Dynamic Systems, 2nd ed. MA: Addison-Wesley, 1990, pp. 222–237.

[5]Fuzzy Logic Toolbox, User's Guide Manual, Version 2. Natick, MA: Mathworks, 2000.

[6]Gilmore, J. P., C. M. Smythe, and S. W. Handford. The effect of l-norepinephrine on cardiac output in the anesthetized dog during graded hemorrhage. *J. Clin. Invest.* 33:884–890, 1954.

[7]Glantz, S. A. Primer of Biostatistics, 4th ed. New York: McGraw Hill, 1997.

[8]Guyton, A. C. Textbook of Medical Physiology, 7th ed. Philadelphia: W. B. Saunders, 1986, pp. 326–335.

[9]Hoeksel, S. A., J. A. Blom, J. R. Jansen, J. G. Maessen, and J. J. Schreuder. Automated infusion of vasoactive and inotropic drugs to control arterial and pulmonary pressures during cardiac surgery. *Crit. Care Med.* 27:2792–2798, 1999.

[10]Huang, J. W., and R. J. Roy. Multiple-drug hemodynamic control using fuzzy decision theory. *IEEE Trans. Biomed. Eng.* 45:213–228, 1998.

[11]Isaka, S., and A. V. Sebald. Control strategies for arterial blood pressure regulation. *IEEE Trans. Biomed. Eng.* 40:353–363, 1993.

[12]Mamdani, E. H., and S. Assilian. An experiment in linguistic synthesis with a fuzzy logic controller. *Int. J. Man-Mach. Stud.* 7:1–13, 1975.

[13]Martin, J. F., A. M. Schneider, and N. T. Smith. Multiple-model adaptive control of blood pressure using sodium nitroprusside. *IEEE Trans. Biomed. Eng.* 34:603–611, 1987.

[14]Meline, L. J., D. R. Westenskow, N. L. Pace, and M. N. Bodily. Computer-controlled regulation of sodium nitroprusside infusion. *Anesth. Analg.* 64:38–42, 1985.

[15]Narendra, K. S., and K. Parthasarathy. Identification and control of dynamic systems using neural networks. *IEEE Trans. Neural Netw.* 1:4–27, 1990.

[16]Nelder, J. A., and R. Mead. A Simplex method for function minimization. *Comput. J.* 7:308–313, 1965.

[17]O'Hara, D. A., D. K. Bogen, and A. Noordergraaf. The use of computers for controlling the delivery of anesthesia. *Anesthesiology* 77:563–581, 1992.

[18]Pajunen, G. A., M. Steinmetz, and R. Shankar. Model reference adaptive control with constraints for postoperative blood pressure management. *IEEE Trans. Biomed. Eng.* 37:679–687, 1990.

[19]Quinn, M. L., N. T. Smith, J. E. Mandel, J. F. Martin, and A. M. Schneider. Automatic control of arterial pressure in the operating room: Safety during episodes of artifact and hypotension? *Anesthesiology* 68:A327, 1988.

[20]Rajfer, S. I., and L. I. Goldberg. Sympathomimetic amines. In: Principles and Practice of Acute Cardiac Care, edited by G. Das and S. Dipankar. Chicago: Year Book Medical, 1984, pp. 126–133.

[21]Rao, R. R., B. Aufderheide, and B. W. Bequette. Experimental studies on multiple-model predictive control for automated regulation of hemodynamic variables. *IEEE Trans. Biomed. Eng.* 50:277–288, 2003.

[22]Rao, R. R., B. W. Bequette, and R. J. Roy. Simultaneous regulation of hemodynamic and anesthetic states: A simulation study. *Ann. Biomed. Eng.* 28:71–84, 2000.

[23]Rao, R. R., J. W. Huang, B. W. Bequette, H. Kaufman, and R. J. Roy. Control of a nonsquare drug infusion system: A simulation study. *Biotechnol. Prog.* 15:556–564, 1999.

[24]Rumelhart, D. E., G. E. Hinton, and R. J. Williams. Learning representations by back-propagating errors. *Nature* 323:533–536, 1986.

[25]Rumelhart, D. E., G. E. Hinton, and R J Williams. Learning internal representations by error propagation. In: Parallel Distributed Processing, Vol. 1, edited by J. L. McClelland, D. E. Rumelhart, and The PDP Research Group. Cambridge, MA: MIT Press, 1986.

[26]Schaer, G. L., M. P. Fink, and J. E. Parrillo. Norepinephrine alone versus norepinephrine plus low-dose dopamine: Enhanced renal blood flow with combination pressor therapy. *Crit. Care Med.* 13:492–496, 1985.

[27]Sheppard, L. C. Computer control of the infusion of vasoactive drugs. *Ann. Biomed. Eng.* 8:431–444, 1980.
[28]Stern, K. S., H. J. Chizeck, B. K. Walker, P. S. Krishnaprasad, P. J. Dauchot, and P. G. Katona. The self-tuning controller: Comparison with human performance in the control of arterial pressure. *Ann. Biomed. Eng.* 13:341–357, 1985.
[29]Sugimachi, M., T. Imaizumi, K. Sunagawa, Y. Hirooka, K. Todaka, A. Takeshita, and M. Nakamura. A new method to identify dynamic transduction properties of aortic baroreceptors. *Am. J. Physiol.* 258:H887–H895, 1990.
[30]Takahashi, Y. Adaptive predictive control of nonlinear time-varying system using neural network. *IEEE Int. Conf. Neural Netw.* 3:1464–1468, 1993.
[31]Tarazi, R. C. Sympathomimetic agents in the treatment of shock. *Ann. Intern. Med.* 81:364–371, 1974.
[32]Trajanoski, Z., and P. Wach. Neural predictive controller for insulin delivery using the subcutaneous route. *IEEE Trans. Biomed. Eng.* 45:1122–1134, 1998.
[33]Waller, J. L., and J. V. Roth. Computer-controlled regulation of sodium nitroprusside infusion in human subjects. *Anesthesiology* 63:A192, 1985
[34]Woodruff, E. A., J. F. Martin, and M. Omens. A model for the design and evaluation of algorithms for closed-loop cardiovascular therapy. *IEEE Trans. Biomed. Eng.* 44:694–705, 1997.
[35]Zadeh, L. A. Making computers think like people. *IEEE Spectr.* 8:26–32, 1984.
[36]Zieglar, J. G., and N. B. Nichols. Optimum settings for automatic controllers. *Trans. ASME* 64:759–768, 1942.